Remote sensing Technology (MODIS) for Extraction Sea surface Salinity Season Variation: Red Sea Saudi Arabia(*)

Dr. Nasser Saeed Jaber Al-Zbnah
Associate Professor of GIS
King Khalid University

Abstract

Sea Surface Salinity model has been applied for high-intensity, short-duration SSS estimation, classification and mapping of SSS from MODIS Satellite data, which are in turn useful for fish potential zone mapping and forecasting, marine management, and improved contingency planning provided that more detailed geophysical studies are concurrently implemented. The outputs of this study are also important for early warning when it is foreseen that unfavorable changes in oceanographic conditions that can affect fish catch may happen. MODIS data demonstrates the ability of signature value in quantifying and predicting the relationships between these parameters, and will so help track the changes in these parameters from time to time for early warning in case of any non-desirable foreseen changes in any or all of these parameters. This type of model also helps for accurate monitoring of large coverage areas at low cost and within short periods of time. Such model furthermore allows prediction of the total fish catch in the different seasons, thus contributing to fish industry management and marketing. This research recommends use of the generated SSS map for mass scale fish harvesting in short time from large areas. The SSS map was carried out off the Yanbu and Jeddah cost of Red sea, Saudi Arabia as there was sufficient In-situ SSS data for accuracy assessment. The Roˆ was computed as 0.92 and the higher SSS have coincided very well with the higher SSS value, meaning the tool is ready for use for extraction salinity and chlorophyll.

Keywords*—Remote sensing; SSS; oceanography; salinity; Sea Surface; MODIS*

استخدام تقنية الاستشعار عن بُعد (MODIS) لقياس تفاوت نسب الملوحة الموسمية في سطح البحر الاحمر، المملكة العربية السعودية

د. ناصر سعيد آل زبنه
استاذ نظم المعلومات الجغرافية المشارك - جامعة الملك خالد

الملخص: تم تطبيق نموذج ملوحة سطح البحر على الكثافة العالية والتقديرات قصيرة الاجل لنسبة ملوحة البحر بالإضافة إلى تصنيف ورسم خرائط نسب ملوحة البحر باستخدام بيانات القمر الصناعي (MODIS)، والتي بدورها تعتبر عامل مساعد في رسم الخرائط المحتملة لوجود الاسماك والتنبؤ بأماكن وجودها، والادارة البحرية، كما كان لها دور في تحسين التخطيط للطوارئ شريطة أن يتم تنفيذ دراسات جيوفيزيائية أكثر تفصيلاً في نفس الوقت. وتعتبر مخرجات هذه الدراسة مهمة ايضاً للحصول على تحذيرات مبكرة عند توقع حدوث تغيرات غير متوقعة في علم المحيطات والتي من الممكن أن تؤثر على صيد الأسماك، وتوضح بيانات موديس MODIS ايضاً قدرة القيمة الرمزية على القياس الكمي وتوقع العلاقات بين كل تلك المعاملات، والمساعدة ايضاً في تتبع التغيرات في تلك المعاملات من وقت إلى آخر بهدف التحذير المبكر من اي تغيرات غير مرغوبة وغير متوقعة في هذه المعاملات. هذا النوع من النماذج يساعد ايضاً على المراقبة الدقيقة جداً لمساحات كبيرة من المناطق المغطاة بتكلفة قليلة وخلال فترات زمنية قصيرة، هذا النوع من النماذج يسمح بالتنبؤ بإجمالي صيد الأسماك في الفصول المختلفة، وتساهم ايضاً في قطاع صيد الاسماك من خلال الادارة والتسويق. يوصي هذا البحث باستخدام خرائط نسب ملوحة سطح البحر المتجددة لإنشاء مقياس ذو نطاق واسع لحصاد الاسماك في بقعة واسعه بأقصر وقت، تم تنفيذ خريطة نسب ملوحة البحر في ينبع وجدة على البحر الاحمر في المملكة العربية السعودية حيث كانت هناك بيانات كافية لنسب ملوحة البحر في تلك المواقع لتقييم دقة هذا النموذج، تم حساب Ro^ على أنه ٠,٩٢ وقد توافقت القيمة الأعلى لنسب ملوحة البحر في تلك المناطق بشكل جيد للغاية مع النسب الأعلى لنسب ملوحة البحر بشكل عام، مما يعني أن الأداة جاهزة للاستخدام في استخلاص الملوحة والكلوروفيل.

الكلمات المفتاحية: الاستشعار عن بُعد، ملوحة سطح البحر، علم المحيطات، الملوحة، سطح البحر، موديس MODIS.

Introduction

A model for extraction of SSS for Red Sea water from MODIS data demonstrates the ability of remote sensing data. Models have used for mapping seasonal distributions of the oceanographic parameters – sea surface salinity (SSS), Although the models are specific for the coastal waters of the study area (Yanbu and Jeddah) they can be used to suit other parts of the Red Sea water. Currently, the coastal zone of Yanbu and Jeddah, has the highest diversity in the marine fish species in the country, including those which are important for the commercial fishing industry. Monitoring salinity and chlorophyll from space, which is regarded as a revolutionary application of remote sensing, started in the last decade. Given this development, remote sensing has potential for monitoring salinity and chlorophyll-a concentration both in the monsoonal and the inter-monsoonal periods. This oceanographic parameter changes continuously due to the effects of natural elements accompanying the different monsoonal and non-monsoonal periods, and these changes in turn affect other oceanographic parameters [7. 9.12.18 and 20].

The SSS and is a key parameters for understanding the global ocean circulation and therefore the role of the oceans in influencing the earth's climate. Together with chlorophyll-a concentration, the SSS affects water density and is hence intimately linked to the horizontal circulation of the oceans and to the depth to which surface water cools in winte1, 2, 3 and 5]. On the other side, the SST is an important component of the thermohaline circulation and is therefore directly linked to the dynamics of the earth's climate [4.6.8 and 10]. In most Middle East countries including Saudi Arabia, mapping SSS and chlorophyll-a is still conducted using ground hydro equipment. The new challenge confronting remote sensing is to retrieve reliable information on changing SSS and chlorophyll-a concentration through the concomitant changes in the spectral properties of the sea surface

Information on the changing oceanographic conditions is necessary

for us to understand, and eventually predict, the effects of these conditions on the fish populations [11, 13, 14, and 16]. In this context, the use of satellite remote sensing to provide synoptic measurements of the oceans is becoming increasingly important in fishery research and fishing operations. Satellite data sets have been used to detect oceanographic parameters such as salinity, temperature front, ocean color, upwelling and chlorophyll concentration as indicators of potential areas for fish congregation and migration [15,17,19].

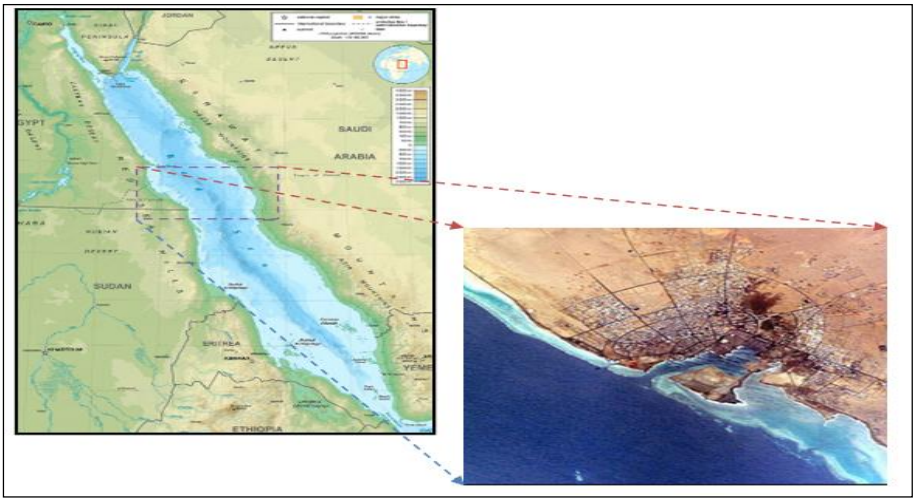

Figure 1. Study area location, Red Sea, Saudi Arabia.

The previous works provided a general description of ocean variability in different sub-regions. Satellite-driven ocean parameter estimation and marine applications of satellite data have been stated in various works, e.g., ocean salinity monitoring using a dual-frequency [6, 9,4 and 20], and using AVHAR mapped potential fish zoning [5,9,8]; and Sea WIFS estimation of SSChll-a and SST [3,12,16,17]. Nonetheless, no published works in the literature investigating variations in the ocean parameters SSS, SST, and Chlorophyll-a concentration in relation to mapping of potential fish zones using MODIS data interpretation are until now found for Red Sea water [17].

MATERIAL AND METHOD

1.1. Study Area Location

The study area stated in (Yanbu and Jeddah), Red Sea, Saudi Arabia, which is located and lies between longitudes 37°59'30.03" N and latitudes 24° 2'57.36" E. Meteorological data indicated that the skies of Red Sea, (Yanbu and Jeddah) have lower cloud density. This is an important observation as MODIS sensors are very sensitive to cloud covers. So, areas of no or low cloud density are more preferred for oceanographic research using MODIS data sets.

1.2. Research Data

1.2.1. Ground Data.

In situ measurements were conducted through sea cruises for a year between 2015 and 2016 along the Yanba, Red Sea, Saudi Arabia. 63 sampling locations for each season were chosen to study coastal Red Sea (Yanba and Jeddah) in the Saudi Arabia. The cruises covered a large-scale area, exceeding 40 km, in 7 months. The Sea cruises were also conducted along the coastal waters of Jeddah from March 2016 to April 2017.

SSS measurements were made off the coasts of Yanba and Jeddah using Hydro lab Troll 9000, while SSChll-a concentration samples were obtained in triplicates of vertical haul chosen at different transects using Hydro lab Datasonde multi-parameter water quality sensor from HACH, USA during the day, as show in figure 2. Samples were fixed with 5% formaldehyde and buffered with borax.

Figure 2. A Hydro lab Sonde Secured with Rope and Data Cable.

Water quality measurements were done off the coast of Yanba,

Jeddah, using a Hydrolab Datasonde multi-parameter water quality sensor from HACH, USA as shown in Figures 2. The instruments were set up to record water quality measurements in real-time mode and the results could be displayed on the computer screen. The parameters recorded are listed in Table 1.

Table 1: Units of the water quality parameters of concern (1) orp: the oxidation-reduction potential.

Ite	Parameter	Unit
1	Conductivity	mS/cm
2	Temperature	Celsius
3	Depth	Meter
4	Salinity	Ppt
5	Ph	
6	ORP(1)	mV
7	Dissolved oxygen	mg/L
8	Turbidity	NTU
9	Chlorophyll-a	ug/L

1.2.2. Satellite Data

In terms of satellite oceanography, several ocean sensors have been launched: the NOAA and Sea-viewing Wide Field-of-view Sensor (SeaWIFS) in July, 1997; Moderate Resolution Imaging Spectroradiometer AM (MODIS AM) in December, 1999; and MODIS PM in May, 2002 (NASA, 2006). The profiling reflectance radiometer (spectroradiometer) has three of MODIS wavelength bands: band 9 (438-338 nm), band 11(526-536 nm), and band 12 (546-556 nm).

The primary remotely-sensed data used in this study were obtained from the MODIS Website, which has been acquiring MODIS data by means of a MODIS Terra and aqua instrument since March 2016, At the same time In-Situ measurement was conducted. MODIS data is multi-spectral, 36-band with high spatial resolution constituted from two 250-m bands, five 500-m bands, and 29 bands of 1-km resolution.

The data is more useful and is more accurate for estimation of ocean parameters SSS and SSchll-a than the Sea WIFS and L-band (Nilhan, 2005). Moreover, they provide high area coverage thus offering a good chance for studying the changing patterns of the ocean parameters. Though, the MODIS data have the limitations of being very sensitive to clouds and that they usually have striping which affects the estimation of ocean parameters.

1.3. Extraction Sea surface salinity (SSS) from MODIS DATA

An existing SSS algorithm deemed suitable for the study site was applied to 27 MODIS scenes for the extraction of SSS using ERDAS window technique based on the radiance-MOD27 S.D algorithm to estimate SSS equations (1-2) [17] in order to get more accurate result we did modification in the existing S.D retrieval SSS model in term of error estimation we reaccount the equation with total error of estimation salinity was accounted when applied S.D model as presented in equation 2. The details of the conceptual model are presented below. This existing SSS retrieval model was using Band 8 to Band16 of MODIS, It is known that the primary usage of Band 8 to Band16 is for ocean color and biogeochemistry observations. The equation used was:

$$S\hat{S}S_1 = \alpha_\circ + \alpha_1 B_{11} + \alpha_2 B_{12} + \cdots + \alpha_P B_{1P} + e_1 = \alpha_\circ + \sum_{j=1}^{P} \alpha_j B_{1j} + e_1. \quad (1)$$

for $1, 2 \ldots \ldots . . n$ and $J = 1, 2 \ldots \ldots . . n$

$S\hat{S}S_n$= predicted value of salinity.

B_{nP}= value of P^{th} predictor of P^{th} value of band n

$\alpha_\circ$= regression constant.

α_P= coefficient on P^{th} predictor.

P = Total number of predictors.

$$SSS_{psu} = (17.321 - 321.3\ \text{Band 6}) - (84.3\ \text{x Band 7}) + (143.132\ \text{band 8}) + (547.892 \times \text{B}and\ 9) + (54.765 \times Band\ 10) - (9.134 \times Band\ 11) - (43.134 \times Band\ 12 \pm bre_n) \quad (2)$$

bre_n = Error term.

II.Result and discussion

2.1. *The Seasonal Variation Of SSS For Red Sea Waters From Modis Image***.**

A total of 24 scenes, meaning two scenes per month, were acquired for the analysis. The monthly average SSS values for the Red Sea waters were computed and the detailed results of SSS seasonal variation are shown in Table 2.

Table 2. The minimum and maximum SSS values for red sea waters from January to December of 2015

Date of Satellite Image	Near Shore SSS (psu)		Open Sea SSS (psu)	
	Min	Max	Min	Max
12th Jan. 2015	34.69	35.45	35.66	36.35
16th Feb. 2015	35.14	35.41	35.12	36.78
19th March 2015	34.95	36.67	35.56	37.52
28th April 2015	35.82	36.11	37.45	38.89
27th May 2015	35.95	36.33	37.23	38.90
28th June 2015	36.76	37.56	38.14	38.89
15th July 2015	36.88	37.45	38.98	39.90
29th August 2015	36.65	37.10	38.25	39.01
23th September 2015	36.10	37.06	37.78	38.90
23th October 2015	36.02	37.56	37.34	38.73
17st November 2015	35.06	36.65	36.89	37.86
12nd December 2015	34.56	35.09	36.24	36.77

2.1.1. The SSS for Red Sea waters from MODIS Image during winter season variation.

Figures 3.1-3.5 show the MODIS-derived SSS distribution maps of the Yanba and Jeddah water in particular and of Red Sea in general for the months of May, June, July, August and September, 2015, respectively, during the SW monsoon and for October inter-monsoon. It is observed that the concentration of SSS was generally higher in the south coast compared to the north coast of Red Sea, particularly in the months of August and September. The influence of the winter season on geophysics parameters is minimal over Red Sea as it is situated in the rain shadow region of the midterm sea Range. The higher SSS in the west coast is attributed to the much calmer sea along the Straits of bab almadeb compared to the much rougher sea off the north coast. This is particularly obvious in the open sea compared to near shore and this is also shown in Table 2 for the Yanba and Jeddah area. But again the south coast has registered higher SSS compared to the north coast.

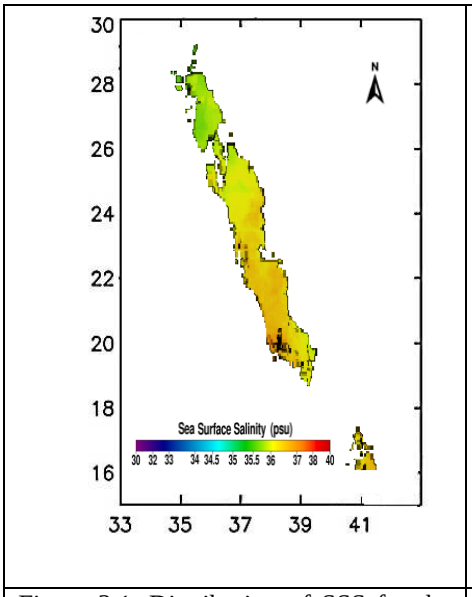

Figure 3.1. Distribution of SSS for the winter season (December, 2014)

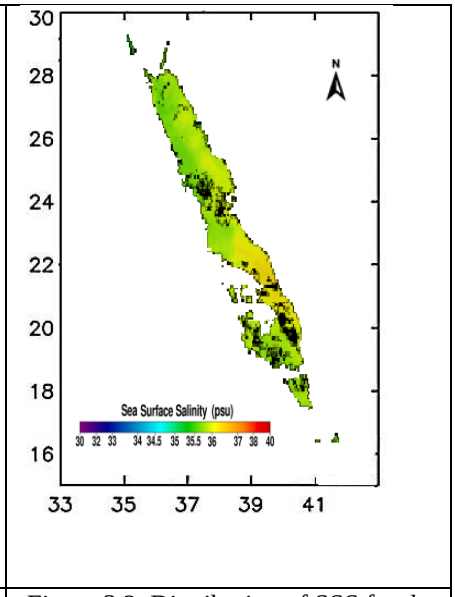

Figure 3.2. Distribution of SSS for the winter season (January, 2015)

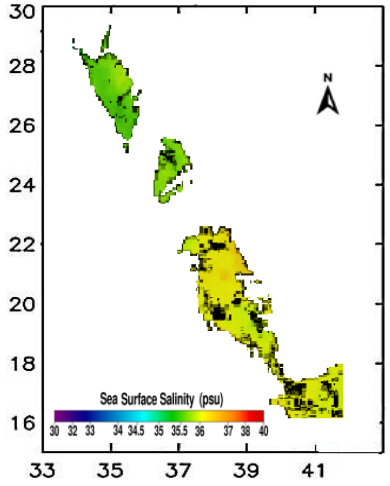

Figure 3.3. Distribution of SSS for the winter season (February, 2015)

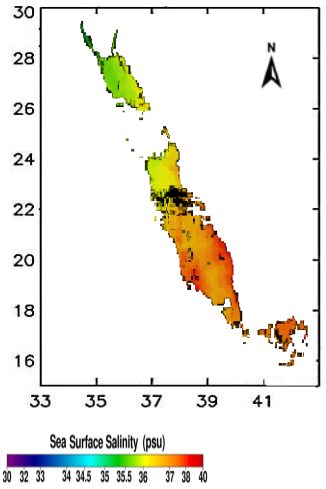

Figure 3.4. Distribution of SSS for the winter season (March, 2015)

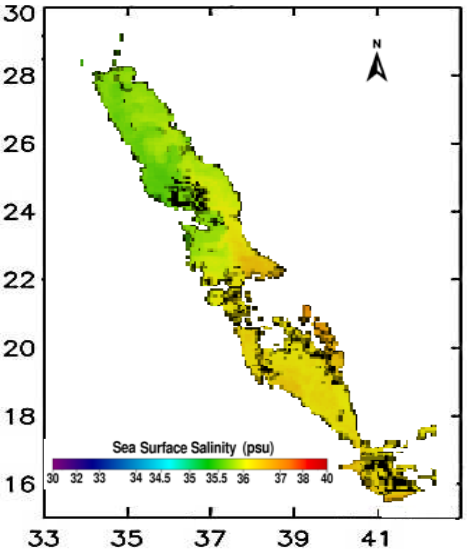

Figure 3.5. Distribution of SSS for Inter-Season Period (April, 2015)

Figures 3.3 and 3.4 show obvious clouds and stripes in the sky of the study area. These lines were generated by the residual differences between MODIS Terra detectors during solar diffuser (SD) calibrations. Figure 3.1 to 3.4 shows the SSS distribution during the

winter season period for January, February, March, and December 2015. It is apparent that the SSS was the lowest during this period due to the high amounts of rainfall during the winter season. Figure 3.5 shows map of early April, 2015, which coplies with a Inter season between winter and summer period and salinity start to be increasing due to began of mild weather. In general, higher SSS values were observed in the north of Red Sea than in the south during the winter than summer.

In general, the SSS distribution pattern shows higher SSS concentrations in the open sea areas during the winter season compared to that of near shore ones due to the amount of fresh water discharge into the near shore from Aden gulf. The open sea SSS varied from the lowest value of 35.12 psu in February to the highest value of 37.52psu, also in March (2015). The near shore SSS varied from the lowest value of 35.12 psu in February to the highest value of 36.67psu in March (2015). However, during the inter-monsoonal priod in April, the SSS varied from the lowest value of 35.82psu in near shore areas to the highest value in open sea of 38.89psu.

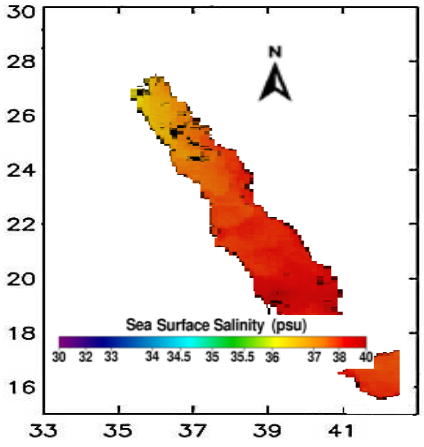

Figure 3.6. The SSS Distribution Map for the summer season in May, 2015

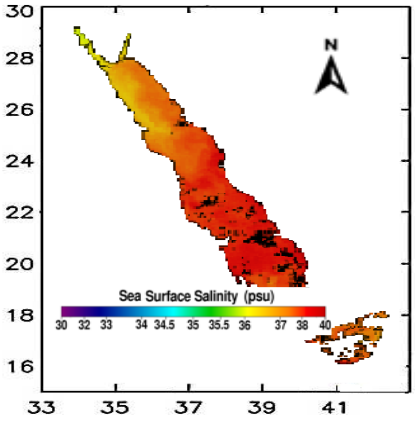

Figure 3.7. The SSS Distribution Map for the summer season in June, 2015

2.2. *The SSS for Red Sea waters from MODIS Image during summer season variation.*

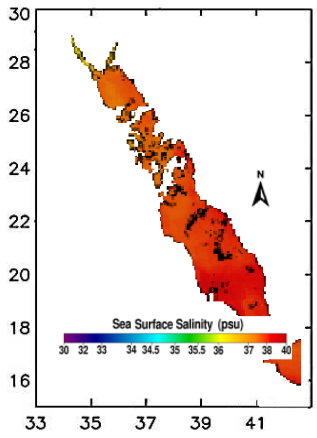

Figure 3.8. The SSS Distribution Map for the summer season in July, 2015

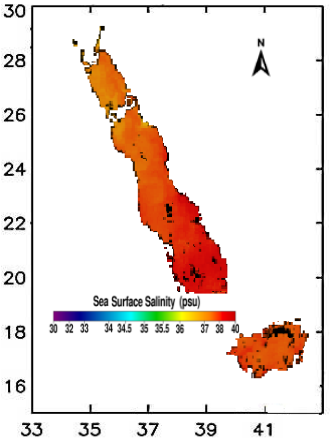

Figure 3.9. The SSS Distribution Map for the summer season in August, 2015.

Stripes in the Figures 3.7-3.8 are clear. These lines were generated by the residual differences between MODIS Terra detectors during solar diffuser (SD) calibrations. Bryan (2007) reported that NASA Ocean Biology Production Group (OBPG) has been trying to reduce the residual detector stripes and reported that the responsiveness of MODIS/Terra sensors degraded up to 40% since its launch.In general, the SSS distribution pattern shows higher SSS concentrations in the open sea areas during the summer season compared to that of near shore ones. The open sea SSS varied from the lowest value of 37.23psu in May 2015 to the highest value of 39.90psu, also in July (2015). The near shore SSS varied from the lowest value of 35.95psu in May to the highest value of 37.45psu in July (2015). However, during the inter-monsoonal period in October and November, the SSS varied from the lowest value of 35.06 psu in November in near shore areas to the highest value in October open sea of 38.73psu.

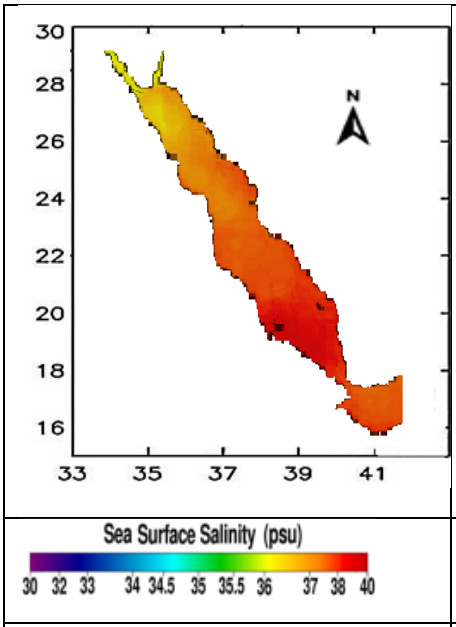

Figure 3.10: The SST Distribution Map for the summer season in September, 2015.

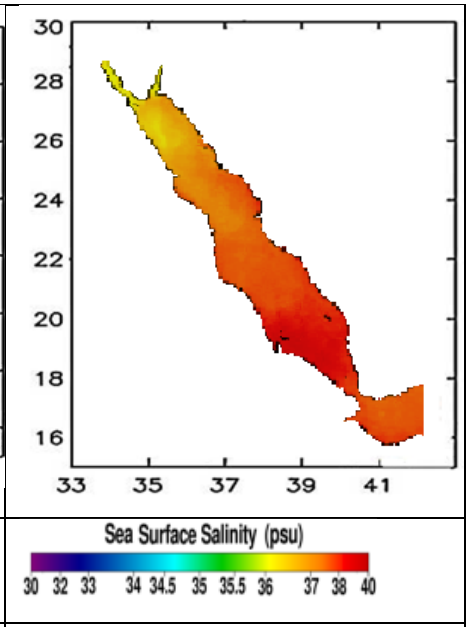

Figure 3.11: The SSS Distribution Map for the autumn season in October, 2015.

Figure 3.11 -3.12 shows the MODIS-derived SSS distribution during the non-monsoonal period in October and November, 2015 wherein the SSS exhibited higher values both in the south and west of Red Sea. Figures 3.1–3.12 show monthly maximum-minimum SSS distributions for both near shore and open sea areas. They indicate that the SSS was low during the winter season (December-March) compared to the summer season (May-September). The low SSS during the winter season was not only due to the monsoonal effect but also to more fresh water discharges into the sea particularly through the barka and. This is especially prominent in the near shore water, which in turn will affect fish aggregation.

The higher SSS values during the summer season could be attributed to the cold sea water, particularly off the south and west of red Sea as the area is situated in the rain shadow region. By and large, the salinity off the north of Red Sea is also low compared to other parts of Red Sea.

The average SSS_{max} for open sea and near shore areas during the winter were respectively 34.56psu and 37.52psu, while the highest SSS_{max} for open sea and near shore areas during the summer season were respectively 36.10 psu and 39.90psu, indicating higher values during the summer Monsoon

The lower values of Red Sea near shore SSS_{max} and SSS_{min} during the winter season compared to the summer one could be related to the high intensity of rainfall received in the Red Sea, especially during the months of December, January, February, and March. This resulted inhigher current speed and inland fresh influx to the near shore areas.

2.3. **Validation of SSS model measurement Vs In-situ measurement**.

In order to evaluate the accuracy of existing SSS models the validations done, the researcher evaluated the RMSE between grond data and model results. This approach has additionally enabled comparison of the results of the *In-situ* with those of those existing models employed in the study.

ERDAS Modeler was used to run the model. Derivation of sea surface salinity (SSS) from the imagery radiance values was implemented following an empirical approach. However, due to the large differences in cloud cover percentages in the images which belong to different times, and ence weathers, a pre-processing phase was included in the modeling task to extract the observed radiance. Comparisons between the *in situ* and MODIS salinity estimates disclosed that the retrieved salinity had high accuracy as indicated by a RMSE as low as 1.5 ($r = 0.92$, $p < .01$) between the *in situ* and MODIS salinity estimates. Figure 4 shows the validation of the MODIS-extracted SSS values with *in situ* SSS data where after layout of the *in situ* SSS measurements on the relevant MODIS images the former SSS values coincided exactly with the salinity class in the image.

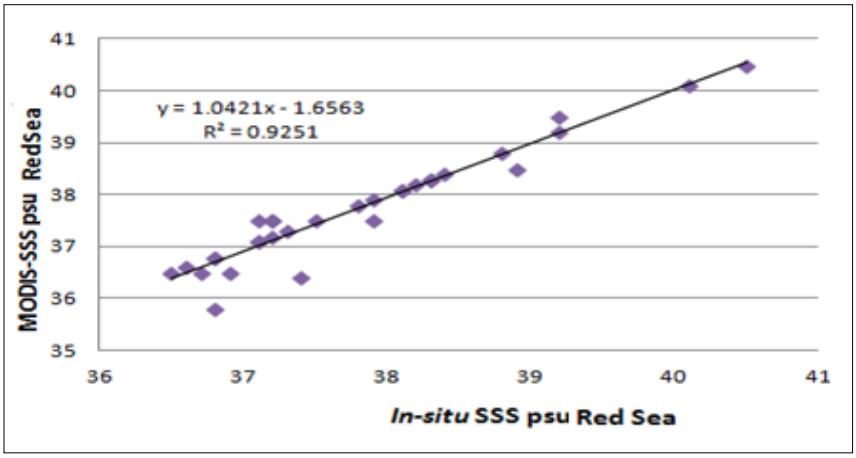

Figure 4. Regression Models between in situ and MODIS-Derived SSS psu Estimates.

CONCLUSIONS

Extraction SSS model has been run using ERDAS Modeler, in order to derive of sea surface salinity (SSS) from the imagery radiance values was implemented following an empirical approach. However, due to the large differences in cloud cover percentages in the images which belong to different times, and ence weathers, a pre-processing phase was included in the modeling task to extract the observed radiance. Comparisons between the *in situ* and MODIS salinity estimates disclosed that the retrieved salinity had high accuracy as indicated by a RMSE as low as 1.5 ($r = 0.92$, $p < .01$) between the *in situ* and MODIS salinity estimates SSS in the south of Red Sea were found to be higher than the respective values in the north part of the Red Sea. The SSS values within the basin vary according to the different environmental conditions attendant to each season. The central part of Red Sea the south part of Red Sea showed high concentrations in the winter (December -March) and late winter monsoon (April), whereas the north part of Red Sea waters had the lowest SSS concentration values in winter. The average SSS_{max} for open sea and near shore areas during

the winter were respectively 34.56psu and 37.52psu, while the highest SSS_{max} for open sea and near shore areas during the summer season were respectively 36.10 psu and 39.90psu, indicating higher values during the summer Monsoon The lower values of Red Sea near shore SSS_{max} and SSS_{min} during the winter season compared to the summer one could be related to the high intensity of rainfall received in the Red Sea, especially during the months of December, January, February, and March. This resulted inhigher current speed and inland fresh influx to the near shore areas.

REFERENCES

1. A. Supply, J. Boutin, J.-L. Vergely, N. Martin, A. Hasson, G. Reverdin, C. Mallet, and N. Viltard, "Precipitation estimates from SMOS sea-surface salinity," Quarterly Journal of the Royal Meteorological Society, Jul. 2017.
2. E. Bayler, "Passive microwave observation spatial biases and uncertainty induced by sea-surface salinity," Oceans11 Mts/ieee Kona, 2011.
3. F. Gaillard, D. Diverres, S. Jacquin, Y. Gouriou, J. Grelet, M. L. Menn, J. Tassel, and G. Reverdin, "Sea surface temperature and salinity from French research vessels, 2001–2013," Scientific Data, vol. 2, p. 150054, 2015.
4. F. Melin, G. Zibordi, and B. N. Holben, "Assessment of the Aerosol Products From the SeaWiFS and MODIS Ocean-Color Missions," IEEE Geoscience and Remote Sensing Letters, vol. 10, no. 5, pp. 1185–1189, 2013.
5. G. Meister and B. A. Franz, "Corrections to the MODIS Aqua Calibration Derived From MODIS Aqua Ocean Color Products," IEEE Transactions on Geoscience and Remote Sensing, vol. 52, no. 10, pp. 6534–6541, 2014.
6. G. Meister, R. E. Eplee, and B. A. Franz, "Corrections to MODIS Terra calibration and polarization trending derived from ocean color products," Earth Observing Systems XIX, Feb. 2014.
7. H. Guo and H. Xie, "Application of MODIS data to monitor sea ice in Bohai sea," 2010 Second IITA International Conference on Geoscience and Remote Sensing, 2010.
8. H. Jiang, M. F. Knudsen, M.-S. Seidenkrantz, M. Zhao, L. Sha, and L. Ran, "Diatom-based reconstruction of summer sea-surface salinity in the South China Sea over the last 15 000 years," Boreas, vol. 43, no. 1, pp. 208–219, Oct. 2013.
9. H. L. Dantzler, "Dynamic salinity calibrations of continuous

salinity/temperature/depth data," Deep Sea Research and Oceanographic Abstracts, vol. 21, no. 8, pp. 675–682, 1974.

10. H. Lu, Y. Li, R. Yu, A. Jin, and R. Lv, "A l-band phased array radiometer for sea surface salinity," 2017 IEEE International Geoscience and Remote Sensing Symposium (IGARSS), 2017.
11. J. P. Boyle, "A surface contact drifter for measurement of near-surface salinity, temperature and sea state," 2012 Oceans, 2012.
12. N. F. Yunita and M. Zikra, "Variability of Sea Surface Temperature in Indonesia Based on Aqua Modis Satellite Data," IPTEK Journal of Engineering, vol. 3, no. 3, 2017.
13. R. Arnone, S. Ladner, G. Fargion, P. Martinolich, R. Vandermeulen, J. Bowers, and A. Lawson, "Monitoring bio-optical processes using NPP-VIIRS and MODIS-Aqua ocean color products," Ocean Sensing and Monitoring V, Mar. 2013.
14. R. Cavalli, "Comparison of Split Window Algorithms for Retrieving Measurements of Sea Surface Temperature from MODIS Data in Near-Land Coastal Waters," ISPRS International Journal of Geo-Information, vol. 7, no. 1, p. 30, 2018.
15. R. Sabia, A. Camps, C. Gommenginger, and M. Srokosz, "Retrieved sea surface salinity spatial variability using high resolution data within the soil moisture and ocean salinity (SMOS) mission," 2007 IEEE International Geoscience and Remote Sensing Symposium, 2007.
16. S. Qing, J. Zhang, T. Cui, and Y. Bao, "Retrieval of sea surface salinity with MERIS and MODIS data in the Bohai Sea," Remote Sensing of Environment, vol. 136, pp. 117–125, 2013.
17. S. T. Daqamseh, S. Mansor, B. Pradhan, L. Billa, and A. R. Mahmud, "Potential fish habitat mapping using MODIS-derived sea surface salinity, temperature and chlorophyll-a data: South China Sea Coastal areas, Malaysia," Geocarto International, vol. 28, no. 6, pp. 546–560, 2013.

18. W. Tang, S. Yueh, A. Fore, and A. Hayashi, “L-band microware signature variation with sea surface temperature and its implication on aquarius sea surface salinity retrieval,” 2017 IEEE International Geoscience and Remote Sensing Symposium (IGARSS), 2017.
19. X. Yu, B. Xiao, X. Liu, Y. Wang, B. Cui, and X. Liu, “Retrieval of remotely sensed sea surface salinity using MODIS data in the Chinese Bohai Sea,” International Journal of Remote Sensing, vol. 38, no. 23, pp. 7357–7373, Nov. 2017.
20. Anas M. Al-Oraiqat, Evgeniy A. Bashkov, V. Babkov & C. Titarenko, “Fusion of Multispectral Satellite Imagery Using a Cluster of Graphics Processing Unit,” International Geoinformatics Research and Development Journal (IGRDJ), Vol. 4, Issue 2, June 2013.